This exam has a total of 100 available points. It is based on the accompanying paper by McIntosh et al. (2011), 'Alfenic waves with sufficient energy to power the quiet solar corona and fast solar wind', Nature, 475, 477. A grade of 70% is expected to be a passing grade.

Calculators are only to be used for calculations. Attempt all parts of all 5 questions.

Constants and Equations.

Equation for material time derivative:

$$\frac{D}{Dt} = \frac{\partial}{\partial t} + \mathbf{v} \cdot \nabla$$
 where **v** is velocity, t is time

Ideal gas law:

$$p = \frac{\rho RT}{\tilde{\mu}}$$

where p is pressure , ρ is mass density, R, the gas constant is 8.3e3 m²s⁻²K⁻¹ T is temperature $\tilde{\mu}$ is the mean atomic weight, =0.6 in the corona

Solar gravitational constant, g = 274 ms-2

Equation for radiative energy losses can reduced to: $E_{rad} = 10e-35 \text{ n}^2$ in the corona where n is the volume density

Proton mass = 1.67e-27 kg

1AU = 1.5e11 m

1: The coronal heating problem

As paraphrased from the paper abstract, an energy flux of 100-200 W m⁻² is required to drive the fast solar wind and balance the radiative losses of the quiet corona. One estimate of this energy flux can be calculated by integrating the radiative loss function over a pressure scale height under magnetostatic equilibrium.

(a) The general form for Newton's 2nd law in a fully ionized plasma is given as the sum of a pressure gradient, a Lorentz force, and a gravitational force.

$$\mathbf{F} = -\nabla p + \mathbf{j} \times \mathbf{B} + \rho \mathbf{g} = \rho \frac{D\mathbf{v}}{Dt}$$

where F is Force, p is pressure, j is current density, B is magnetic field strength. Consider that both B, p, and g only vary in the vertical direction (z). Show that in the case of magnetostatic equilibrium this can be reduced to a first order ordinary differential equation of the form.

$$\frac{dp}{p} = -\frac{1}{H(z)}dz.$$

where H is pressure scale height,

$$H(z) = \frac{RT(z)}{\tilde{\mu}g}$$

Be sure to state the assumptions necessary.

(15 marks)

(b) Integrate the ODE above to show that H is simply the height over which the pressure decreases by an exponential factor.

(10 marks)

- (c) For typical coronal values, show this pressure scale height is on the order of the heights of the loops in Fig 3 (Estimate footpoint separation and assume a semicircular geometry). Comment on the viability of the assumption of magnetostatic equilibrium for coronal structure.

 (10 marks)
- (d) The energy flux can be calculated as the radiative energy losses integrated over one scale height (i.e, Flux = Radiative energy loss X Pressure scale height). Show the energy flux required to balance radiative losses is on the order of the values quoted in the paper. State two other types of energy losses that have not been considered in this calculation.

(5 marks)

2: Instrumentation

(a) Calculate the spatial resolution (in Km) of the SDO AIA telescope in the Fe IX passband (see pg 477; left column). The telescope had a 20cm diameter.

10 marks)

(b) Why is this value different from the spatial resolution of 870 Km as quoted in the paper. (pg 477; left column.)

(5 marks)

3: Methods

(a) In order to calculate the phase speeds (end of first page), the authors carry out a cross correlation of the emission at a separation of 3 pixels. For the phase speeds stated in this paper, over what time does the wave move a distance of 3 pixels.

(10 marks)

(b) Comment on the validity of such a measurement when compared to the original cadence and, assuming the measurement is is correct, how could the validity of the measurement be enhanced.

(5 marks)

4: Results

In the quiet Sun and coronal holes the authors state that 'the observed phase speeds and densities are compatible with the presence of magnetic fields of the order of 10G. '

(a) The Alfven speed is directly proportional to the ambient magnetic field strength and inversely proportional to the square root of the mass density. State this phrase in the form of an equation for both the "quiet Sun" and "active regions".

(5 marks)

(b) Combine the two equations from 4(a) to calculate the typical magnetic field strength in active regions. Typical coronal densities in active regions are an order of magnitude greater than quiet Sun or coronal holes.

(15 marks)

5: Future work

The authors state that 'higher spatial and temporal resolution are required to study the full spectrum of wave energy in active regions, because of the smaller length and shorter periods that are likely to exist there'. Such statements can be quantified by noting the available komega phase space for the instrument and noting the area in this phase space where the physics occurs. k is the spatial wavenumber, and omega is the angular frequency

Sketch a set of k against omega axis. Calculate the limiting (maximum) values of k and omega which can be achieved by the SDO AIA instrument (from the spatial and temporal resolution of the instrument). Note which part of the phase space in your plot cannot be studied by drawing vertical and horizontal lines at these limiting values and shading the region of the graph where SDO AIA cannot probe.

Show that quiet Sun (k=0.0063 km-1, omega = 0.04Hz) lies in the available phase space and that active regions (k=0.011km-1, omega=0.063Hz) does not lie in the available phase space.

(10 marks)

LETTER

Alfvénic waves with sufficient energy to power the quiet solar corona and fast solar wind

Scott W. McIntosh¹, Bart De Pontieu², Mats Carlsson³, Viggo Hansteen^{2,3}, Paul Boerner² & Marcel Goossens⁴

Energy is required to heat the outer solar atmosphere to millions of degrees (refs 1, 2) and to accelerate the solar wind to hundreds of kilometres per second (refs 2-6). Alfvén waves (travelling oscillations of ions and magnetic field) have been invoked as a possible mechanism to transport magneto-convective energy upwards along the Sun's magnetic field lines into the corona. Previous observations7 of Alfvénic waves in the corona revealed amplitudes far too small (0.5 km s⁻¹) to supply the energy flux (100-200 W m⁻²) required to drive the fast solar wind8 or balance the radiative losses of the quiet corona9. Here we report observations of the transition region (between the chromosphere and the corona) and of the corona that reveal how Alfvénic motions permeate the dynamic and finely structured outer solar atmosphere. The ubiquitous outward-propagating Alfvénic motions observed have amplitudes of the order of 20 km s⁻¹ and periods of the order of 100-500 s throughout the quiescent atmosphere (compatible with recent investigations7,10), and are energetic enough to accelerate the fast solar wind and heat the quiet corona.

In the chromospheric region, just above the solar photospheric surface but below the corona, observations from the Hinode space-craft! revealed the presence of Alfvénic (Supplementary Information) waves that have significantly higher amplitudes (20 km s⁻¹) than in the corona (0.5 km s⁻¹). The chromospheric waves were observed on spicules¹⁰, which are jet-like features at the solar limb that protrude into the hot corona^{12,13}. The apparent discrepancy between the chromospheric and coronal measurements^{2,10} has raised concerns that these low-frequency Alfvénic motions do not contribute significantly to the energy balance of the outer solar atmosphere and inner heliosphere, perhaps because the large chromospheric wave energy flux is dissipated or reflected before reaching the corona.

Previous reports of Alfvén waves in the coronal plasmas⁷, which are at temperatures of ~10⁶ K, were based on measurements of line-of-sight (Doppler) velocity or, more indirectly, on non-thermal line broadening of spectral lines at lower spatial (~4.5 Mm) and temporal (30 s) resolution. Here we use the He II 304-Å and Fe IX 171-Å channels of the Atmospheric Imaging Assembly (AIA¹⁴) on board the Solar Dynamics Observatory (SDO) satellite to make observations of the solar transition region and of the corona. The spatial resolution (~870 km on the Sun) and temporal resolution (8 s) available allow us to directly image the transverse swaying of magnetic field lines as Alfvénic waves pass through plasma at ~10⁵ K (in the transition region) or at coronal temperatures.

Movies of the 304-Å channel at the solar limb show a transition region that is dominated by spicular jets that shoot rapidly (20–150 km s⁻¹) upwards, often reaching heights of 20,000 km above the solar limb (Supplementary Movie 1). Movies of the same region in the 171-Å channel reveal coronal disturbances that propagate outward at high speeds (100–200 km s⁻¹; Supplementary Movie 2). Recent analysis 15 has showed that these spicules and propagating disturbances are the transition-region and coronal counterparts of the chromospheric spicules 10,13,16, illustrating

that those spicules are associated with material that is heated to coronal temperatures. These transition-region and coronal features undergo significant Alfvénic motion, with displacements varying sinusoidally in time (Fig. 1, Supplementary Movies 1-4). Because the magnetic field dictates the direction of plasma motions at these heights of the solar atmosphere, the observed transverse (to the long axis of the ejected material) motions imply the presence of Alfvénic waves.

The SDO/AIA image sequences show a hot outer atmosphere that is replete with Alfvénic waves (Fig. 2; Supplementary Movies 1--7). The waves are traced by structures that do not have particularly long lifetimes (of the order of 50-500 s) compared to the wave periods, and are difficult to detect because of the enormous line-of-sight superposition in the atmosphere above the solar limb. To avoid these issues, we use Monte Carlo simulations (Supplementary Information) to study the statistical properties of the waves. Below 20 Mm in height, we see a predominance of linear motion and partial swings (as opposed to full swings) in the space-time plots, because of the short transition-region spicule lifetimes. In the hotter corona, extending further from the surface, the spicule-related propagating coronal disturbances display a mix of superposition and more complete sinusoidal motions with the same period. This suggests that the motions visible in the transition region and corona share a common origin.

Our Monte Carlo simulations (Fig. 2) show that the observations are compatible with the presence of Alfvénic waves with amplitudes of $25 \, \mathrm{km \, s^{-1}}$ in the coronal hole and $20 \, \mathrm{km \, s^{-1}}$ in the quiet Sun. Visual comparison of the observations and simulations roughly limit the periods to a range between $150 \, \mathrm{and} \, 550 \, \mathrm{s}$: waves with very short periods of the order of $50 \, \mathrm{s}$ or with very low amplitudes ($<15 \, \mathrm{km \, s^{-1}}$) do not fit the data very well (Supplementary Figs 2 and 3). The active solar corona can be analysed using a similar combination of techniques. Figure 3 (and Supplementary Movies 5-7) illustrates that the entire active region complex is riddled with transverse motion. The active region waves have shorter periods ($100-400 \, \mathrm{s}$) and considerably lower amplitudes ($5\pm 5 \, \mathrm{km \, s^{-1}}$). By cross-correlating space–time plots at increasing distance above the limb, or along the coronal loops, we can estimate the phase speed (and associated error; see Supplementary Information) of the observed Alfvénic motions (Fig. 4; Supplementary Movies 3 and 4).

Using the wave amplitude inferred from our Monte Carlo simulations ($v = 20-25 \, \mathrm{km \, s}^{-1}$ at a height of 15 Mm) and the phase speeds inferred from cross-correlation of the coronal emission ($V_A = 200-250 \, \mathrm{km \, s}^{-1}$ at the same height), we conservatively estimate the wave energy flux (E_A) present in the coronal hole and quiet Sun regions using the expression $E_A = f \rho v^2 V_A$, where f is the filling factor of the waves, and ρ is the mass density in the each of the solar domains. The cross-field coherence in the oscillating features we observe (Supplementary Figs 4 and 5), and numerical simulations showing pervasive waves throughout the solar atmosphere¹⁰, indicate that these waves are volume-filling ($f \approx 1$; see Supplementary Information). Using order-of-magnitude estimates for the density of wave-carrying features in the

¹High Allitude Observatory, National Center for Atmospheric Research, PO Box 3000, Boulder, Colorado 80307, USA. ²Lockheed Martin Solar and Astrophysics Laboratory, 3251 Hanover Street, Palo Alto, California 94304, USA. ³Institute of Theoretical Astrophysics, University of Oslo, PO Box 1029 Blindern, 0315 Oslo, Norway. ⁴Department of Mathematics, Centre for Plasma Astrophysics, Katholieke Universiteit Leuven, Celestijnenlaan 2008, B-3001 Heverlee, Belgium.

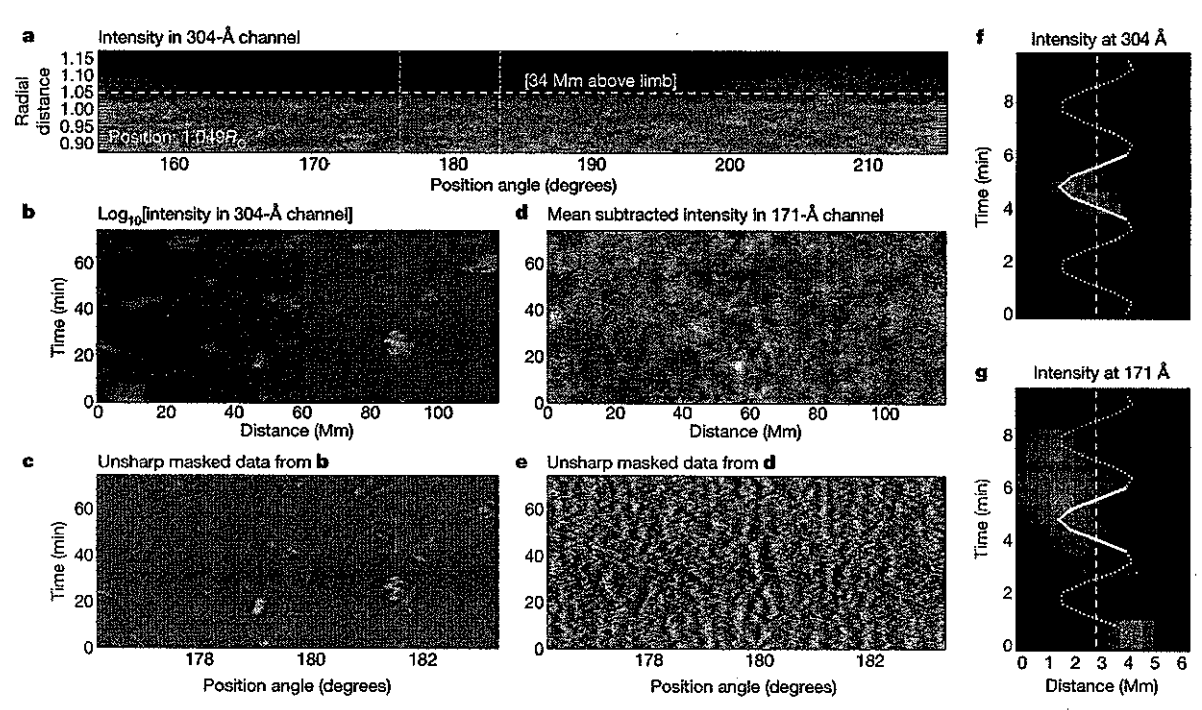


Figure 1 | Ubiquitous Alfvénic motion above the solar limb. Space-time plots of SDO/AIA data, demonstrating the visibility of the ubiquitous transverse waves 34 Mm above the solar limb in a coronal hole. a, Radial distance-position angle map, showing intensity in the 304-Å channel; the location studied is shown by the dashed horizontal line between the two vertical dashed lines. The intensity images (b, 304-Å channel) and mean-subtracted intensity images

(d, 171-Å channel) show a number of oscillatory structures that are enhanced using unsharp masking (c and e, respectively). We highlight one oscillation as an example; it is shown enclosed in a red rectangle, and is compatible with propagation along the spicule (f, 304-Å channel), and with propagating coronal disturbance (g, 171-Å channel). A sine wave with a period of 180 s and an amplitude of $24\,\mathrm{km\,s}^{-1}$ is drawn on f and g as a visual aid for the reader.

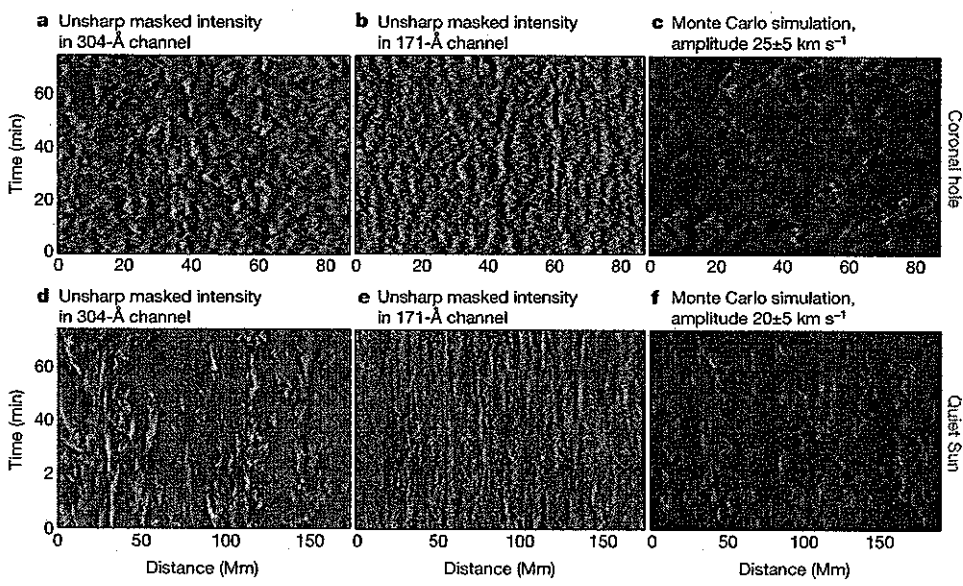


Figure 2 | Examining Alfvénic motion in coronal hole (top row) and quiet Sun (bottom row) regions. a-e, SDO/AIA space-time plots of unsharp masked intensity in the 304-Å (a, d) and 171-Å (b, e) channels 15 Mm above the solar limb (Supplementary Movies 3 and 4). c, f, Monte Carlo simulations for Alfvénic waves with periods of 150-600 s and amplitudes of 25 (±5; c) and 20 (±5; f) km s⁻¹. These simple simulations indicate that the spatio-temporal

superposition of many independent bright features carrying Alfvénic waves with random phases leads to poor visibility of the extrema, or 'swings' of the sinusoidal motion. This is because many of the sinusoidal swings are superimposed on top of features that do not show any apparent lateral motion (the polarization of the Alfvénic wave is along the line-of-sight).

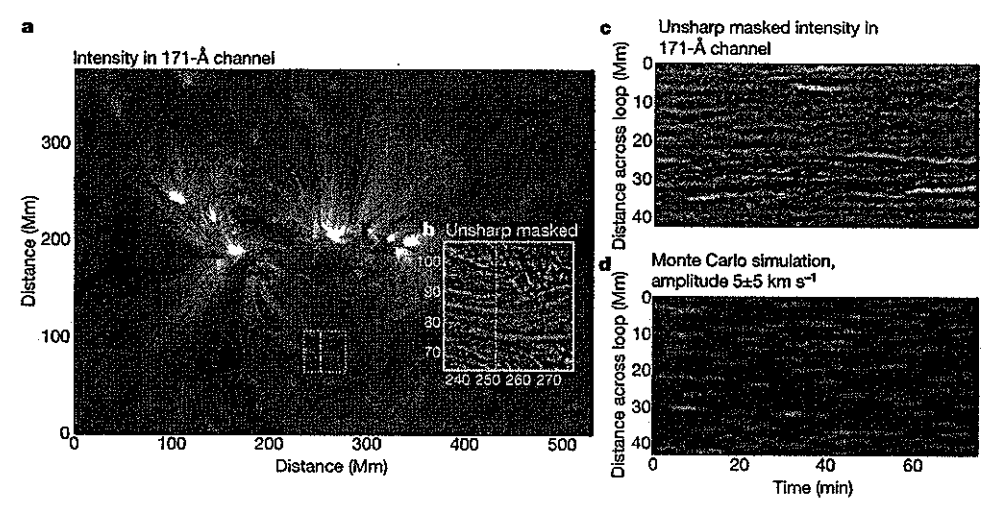


Figure 3 | Examining Alfvénic motion in an active region of the Sun. An active region loop system was observed in the SDO/AIA 171-Å channel (a, taken on 25 April 2010, at 02:00 UT; Supplementary Movies 5-7). By isolating the coronal loops in the study region (boxed in a, shown magnified

and unsharp masked in b), we demonstrate the variation of the signal at one location (the dashed vertical line). From this we produce a space-time plot (c) for comparison with a Monte Carlo simulation (d; amplitude $5\pm 5\,\mathrm{km\,s}^{-1}$, period $100-400\,\mathrm{s}$).

coronal hole and quiet corona $((5-10)\times10^{-13} \text{ kg m}^{-3}; \text{Supplementary Information})$, we determine energy flux densities of the order of $100-200 \text{ W m}^{-2}$ at a height of 15 Mm. The observed phase speeds and densities are compatible with the presence of magnetic fields of the order of 10 G.

The SDO/AIA observations of transition-region and coronal emission have permitted the measurement of the amplitude, period and phase speed of ubiquitous transverse waves. The estimated energy flux is sufficient to provide the energy necessary to drive the fast solar wind⁸ and overcome the radiative losses of the quiet solar corona⁹.

The estimated energy flux of low-frequency Alfvénic waves in denser active region loops (~100 W m⁻²; Supplementary Information) is not sufficient to provide the entire 2,000 W m⁻² required to power the active corona⁹. However, we warn that the phase speed of the disturbances seen in the active corona may be significantly under-reported, because bidirectional waves on the loops¹⁷ can reduce the amplitude and phase speed. Further, we believe that instrumentation of higher spatial and temporal resolution than that of the SDO/AIA are required to study the full spectrum of wave energy (including higher frequencies) in active regions, because of the smaller length scales and shorter period

waves that are likely to exist there (Fig. 3). Therefore, the effect of Alfvénic waves on the energy balance of the active solar corona remains unclear, although our observations suggest that low-frequency Alfvénic waves do not carry enough energy to significantly affect active region heating.

Our results (for the quiet corona and coronal holes) suggest that a 'two-stage' process may be at play in the quiescent solar atmosphere. The first stage is an initial heating and injection of plasma from the lower atmosphere. This is supplemented by the second stage, which involves the dissipation of the Alfvénic waves; this dissipation can sustain the temperatures (~10⁶ K) of the coronal material in the quiet Sun, or accelerate the solar wind in a coronal hole. Such a secondary energy source in the magnetically closed regions of the corona can explain the gentle, steady evaporation of material from the upper chromosphere and transition region that is driven by downward thermal conduction's, as well as the stark spectroscopic contrast between the two^{19,20}. Although caution is clearly necessary, the scheme we propose may not be too far-fetched: recent observational evidence of dissipation of Alfvénic waves in the quiet corona¹⁷, and many models, suggest that the transfer of energy from low-frequency Alfvénic waves

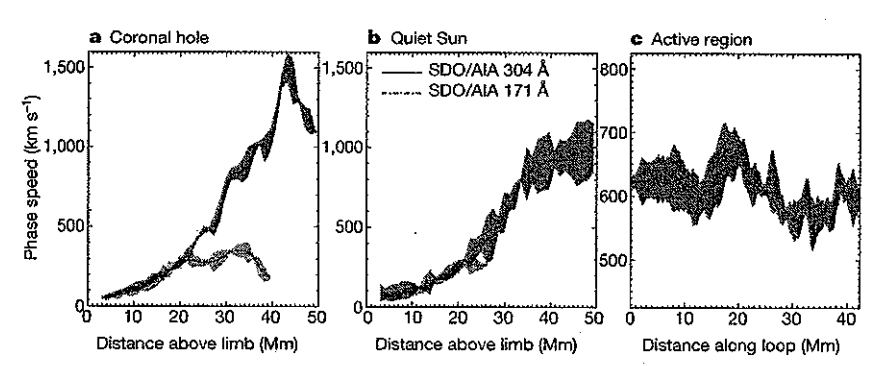


Figure 4 | Determining the phase speed of the Alfvénic motions. By cross-correlating the space-time plots at different heights above the limb, we can measure the phase speed of the observed disturbances and their error computed from an ensemble of cross-correlations about that height (dashed regions; Supplementary Information). Data are shown for coronal holes (a), quiet Sun (b) and along a coronal loop complex in an active region (c). In a and b we show results from both SDO/AIA channels (304 Å and 171 Å; c shows 171-Å results only. We see that the profiles of coronal hole and quiet Sun phase speed

determined from transition region emission rise to $\sim 250\,\mathrm{km\,s^{-1}}$ at a distance of 20 Mm above the solar limb, which is consistent with chromospheric measurements. The continued increase to $\sim 1,000\,\mathrm{km\,s^{-1}}$ at a distance 40 Mm above the limb is consistent with previous coronal phase speed determinations? The phase speed determined for the active region studied is of the order of $600\,\mathrm{km\,s^{-1}}$, and a small variance ($\sim 50\,\mathrm{km\,s^{-1}}$) is observed along the loop structures.



to the plasma is essential to drive the fast solar wind to the high velocities observed at 1 AU (astronomical unit) from the Sun3-5,21-23 The challenge remains to understand how, and where, these waves are generated and dissipated in the solar atmosphere, and how that dissipation delivers energy to the ions and electrons that comprise the coronal plasma and solar wind^{6,23}.

Received 16 February; accepted 25 May 2011.

- Belcher, J. W. & Olbert, S. Stellar winds driven by Alfvén waves. Astrophys. J. 200, 369-382 (1975).
- Axford, W. I. et al. Acceleration of the high speed solar wind in coronal holes. Space Sci. Rev. **87**, 25–41 (1999).
- Matthaeus, W. H., Zank, G. P., Oughton, S., Mullan, D. J. & Dmitruk, P. Coronal heating by magnetohydrodynamic turbulence driven by reflected low-frequency waves. Astrophys. J. 523, L93–L97 (1999).
- Cranmer, S. R., van Ballegooijen, A. A. & Edgar, R. J. Self-consistent coronal heating and solar wind acceleration from anisotropic magnetohydrodynamic turbulence. Astrophys. J. 171 (Suppl.), 520-551 (2007).
- Suzuki, T. K. & Inutsuka, S.-i. Solar winds driven by nonlinear low-frequency Alfvén waves from the photosphere: parametric study for fast/slow winds and disappearance of solar winds. J. Geophys. Res. 111, A06101, doi:10.1029/ 2005JA011502 (2006).
- Verdini, A., Velli, M., Matthaeus, W. H., Oughton, S. & Dmitruk, P. A turbulencedriven model for heating and acceleration of the fast wind in coronal holes. Astrophys. J. 708, L116-L120 (2010).
- Tomczyk, S. et al. Observations of Alfvén waves in the quiet solar corona. Science 317, 1192-1196 (2007).
- Hansteen, V. H. & Leer, E. Coronal heating, densities, and temperatures and solar
- wind acceleration. J. Geophys. Res. 100, 21577–21593 (1995).
 Withbroe, G. L. & Noyes, R. W. Mass and energy flow in the solar chromosphere and
- corona. *Annu. Rev. Astron. Astrophys.* **15**, 363–387 (1977).

 10. De Pontieu, B. *et al.* Chromospheric Alfvénic waves strong enough to power the solar wind. *Science* **318**, 1574–1577 (2007).
- Tsuneta, S. et al. The solar optical telescope for the Hinode mission: an overview. Sol. Phys. 249, 167-196 (2008).
- 12. Beckers, J. M. Solar spicules. Sol. Phys. 3, 367-433 (1968).

- 13. De Pontieu, B. et al. A tale of two spicules: the impact of spicules on the magnetic chromosphere. Publ. Astron. Soc. Jpn 59, 655-662 (2007)
- 14. Lemen, J. R. et al. The Atmospheric Imaging Assembly on the Solar Dynamics Observatory. Sol. Phys. (submitted).

 15. De Pontieu, B. et al. The origin of hot coronal plasma. Science 331, 55–58 (2011).
- 16. De Pontieu, B., McIntosh, S. W., Hansteen, V. H. & Schrijver, C. J. Observing the roots
- De Ponteu, B., McIntosh, S. W., Hansteen, V. H. & Schrijver, C. J. Observing the roots of solar coronal heating—in the chromosphere. *Astrophys. J.* 701, L1–L6 (2009).
 Tomczyk, S. & McIntosh, S. W. Time-distance seismology of the solar corona with CoMP. *Astrophys. J.* 697, 1384–1391 (2009).
 Patsourakos, S. & Klimchuk, J. A. Nonthermal spectral line broadening and the nanoflare model. *Astrophys. J.* 647, 1452–1465 (2006).
 McIntosh, S. W. *et al.* Observations supporting the role of magnetoconvection in energy supply the culter of the culter of the control of the control of the control of the control of the culter of the culter of the control of the culter of the culter of the control of the culter of the culte
- energy supply to the quiescent solar atmosphere. Astrophys. J. 654, 650-664 (2007).
- McIntosh, S. W., Learnon, R. J. & De Pontieu, B. The spectroscopic footprint of the fast solar wind. *Astrophys. J.* 727, 7 (2011).
 Hollweg, J. V. Alfvén waves in a two-fluid model of the solar wind. *Astrophys. J.* 181,
- 547-566 (1973).
- 22. Chandran, B. D. G. Alfvén-wave turbulence and perpendicular ion temperatures in
- coronal holes. Astrophys. J. **720**, 548–554 (2010). 23. Cranmer, S. R. & van Ballegooijen, A. A. Can the solar wind be driven by magnetic reconnection in the Sun's magnetic carpet? Astrophys. J. 720, 824-847 (2010).

Supplementary Information is linked to the online version of the paper at www.nature.com/nature.

Acknowledgements SDO is the first mission of NASA's Living With a Star Program. NCAR is sponsored by the NSF.

Author Contributions S.W.M. (with B.D.P. and M.C.) performed all image processing and analysis of observations. S.W.M. and M.C. calculated phase speeds. P.B. (with B.D.P. and V.H.H.) designed the special observing sequences. B.D.P. co-aligned the data, performed Monte Carlo simulations (with V.H.H.) and provided density estimates. M.G. assisted with the identification of the wave mode. S.W.M. and B.D.P. wrote the manuscript. All authors discussed the results and commented on the manuscript.

Author Information Reprints and permissions information is available at www.nature.com/reprints. The authors declare no competing financial interests. Readers are welcome to comment on the online version of this article at www.nature.com/nature. Correspondence and requests for materials should be addressed to S.W.M. (mscott@ucar.edu).

(9)
$$F = -\nabla p + g \wedge g + eg = e \frac{\partial v}{\partial k}$$

in magnetostable equilibrium $\frac{\partial}{\partial k}$ is zero

(herefore

 $-\nabla p + g + g = 0$

where $B = B(z)$, $g = 0 = 0$ to what $z = 0$

Where $P = P(z)$ and $e = e(z)$
 $\frac{\partial}{\partial z} = -e(z)g$

From ideal $g = 0$
 $\frac{\partial P(z)}{\partial z} = -e(z)g$
 $\frac{\partial P(z)}{\partial z} = -e(z)g$
 $\frac{\partial P(z)}{\partial z} = -e(z)g$

Substitute $G = 0$
 $\frac{\partial P(z)}{\partial z} = -e(z)g$
 $\frac{\partial P(z)}{\partial z} = -e(z)g$
 $\frac{\partial P(z)}{\partial z} = -e(z)g$

Where $\frac{\partial P(z)}{\partial z} = -e(z)g$
 $\frac{\partial P(z)}{\partial z}$

(Erronging (3) $\frac{dP}{P} = -\frac{1}{H}dz$ 16) $\frac{dp}{p} = -\frac{1}{H(2)}d(2)$ Intégrée Fran 200 P=Po 6 202, P=P NR 8 - 1-A(2) dZ MSSLARE 4(3) 15 [m P]Po = -4 10 de constarter starty way 19 In Rose 22 dop expended days His scale height of on H= RT = (8.3e3)(1e) - 1887in ~50e6 250 MM Egge, Consport repeation 100Am En lugar n = height 50 Mm He re consee these loops, ms is problem problem dung Places

= RN X H = (10⁻³⁵)(n²) (50 40°) n's number desily e=5e-13 hgm3 u = (0.6)(167 K(6-77)) 10 N 30 23 A Sell E = (10-35) (25) (1028) (5) (107) = 125 10 38 10 30 =125 WM Not considered: Condition losses accleded public

- (122)(12/6) -(e)(e) 1 le redions = (1e 2/1-Se") ~1.5c 4 215 hm Outed spetial resolution - 5704 m is achely pixel size resolver,

$$d = pixel size = \frac{870}{2} 4m$$

$$250 = \frac{3 \times (\frac{870}{2})}{62}$$

$$62 = 5.25$$

(b) Both t, and to are less than the cadence of t=8s as quoted in the paper. This questions the validity of such a result.

the question $V \prec \frac{3}{\rho''^2}$ From the paper for quiet Sun I carmol holes Vas & Bas VAR & BAR
PAR Divide @ by @ Vas
VAR = (Bas) × (PR) 1/2

(BAR) × (PR) 1/2 From the paper, Fig 4, and text $\frac{200}{600} = \frac{10}{\text{SAR}} \times \left(\frac{\text{CAR}}{5e^{-13}}\right)^{1/2} = 5$ From the question, and by rerranging 19 BAR = 10 × 3 × (Se-12) 1/2 = 30 × 10 ~ 100 G

$$W_{MAX} = 2H V_{MAX}$$

$$= 2H \frac{1}{2\times8}$$

$$= 0.392 H_2$$

$$V_{MAX} = \frac{2H}{2MN}$$

$$= \frac{2H}{850}$$

$$= 0.00739 Km^{-1}$$

